ELSEVIER

Journal of Hazardous Materials 37 (1994) 303–325

JOURNAL OF HAZARDOUS MATERIALS

Movement of chemical warfare agent simulants through porous media

R.A. Jenkins[a,*], M.V. Buchanan[a], R. Merriweather[a], R.H. Ilgner[a], T.M. Gayle[b], A.P. Watson[c]

[a] *Analytical Chemistry Division, Oak Ridge National Laboratory, Building 4500S, MS-6120, P.O. Box 2008, Oak Ridge, TN 37831-6120, USA*

[b] *Instrumentation and Controls Division, Oak Ridge National Laboratory, Oak Ridge, TN, USA*

[c] *Health Sciences Research Division, Oak Ridge National Laboratory, Oak Ridge, TN, USA*

(Received 13 May 1993; accepted in revised form 23 October 1993)

Abstract

A measurement protocol is documented and data presented to characterize the permeation of chemical warfare agent simulants through the porous construction materials brick, cinder block, gypsum wall board, and wood. These data will be used to develop guidelines for access ('reentry') to potentially contaminated properties if nerve or vesicant agents are released during any phase of the US Department of the Army's Chemical Stockpile Disposal Program. A novel permeation cell design allowed sampling of air volumes adjacent to the spiked face, breakthrough face and lateral face of each test medium at two temperatures. Simulant movement through wood is nearly always in the direction of the wood grain. Two-dimensional breakthrough was observed in brick and gypsum wall board. The sulfur mustard simulant broke through all test media in less than 60 min; nerve agent simulant breakthrough required several hours. Surface decontamination of wood with high test hypochlorite is 95% effective.

1. Introduction

The Chemical Stockpile Disposal Program of the US Department of the Army was mandated by the US Congress in 1985 (PL 99-145) to destroy the US retaliatory stockpile of lethal unitary chemical agents and munitions. The program and warfare agent toxicity are more fully described in Carnes and Watson [1], Carnes [2, 3], Watson et al. [4], and others. Briefly, the agents scheduled for destruction are the organophosphate (OP) ('nerve') agents GA (tabun), GB (sarin) and VX; and the vesicant ('blister') agents H, HD, HT (various formulations of sulfur mustard) and

* Corresponding author.

SSDI 0304-3894(93)E0106-C

Lewisite (an organic arsenical). Nerve agent VX and the sulfur mustard blister agent formulations were designed to be persistent under environmental conditions and are therefore problematic in terms of planning for reentry, restoration and recovery of locations that may become contaminated during continued storage or any stage of the disposal program [5]. This issue has been partly addressed for agricultural resources in the paper by Buchanan et al. [6].

There are presently no criteria suitable for designating potentially contaminated masonry, wood, wallboard or other 'porous media' as free of hazardous agent concentrations. Concepts that have been previously considered include treating the suspect item or surface as if it were a piece of military hardware being prepared for sale to the public as scrap [7], wipe sampling of the suspect surface, or enclosing the item or area in an airtight manner followed by surface heating and airstream sampling. There are sampling and interpretation problems inherent to each of these approaches, not the least of which is how to determine acceptable agent concentrations for conditions of unlimited public access. The military scrap guidelines are the only US standards governing agent decontamination of material that can be released to the public; they were never intended for application to the treatment of public or private property under civilian, not military, control.

Most military guidelines for reentry and reuse of resources and material exposed to agent liquid or long-term agent vapor contamination are primarily mission-oriented for application under combat conditions or post-attack occupation. As such, these guidelines seek to limit personnel exposure by decontaminating often-used items such as weapons, ammunition, hatches and seats of vehicles, etc., rather than eliminating all traces of agent on any part of the item [8].

The study reported below is designed to assess the degree of sorption of agent simulants into, and permeation through, construction materials at two temperatures. In addition, the likelihood of simulant offgassing after application of established decontamination procedures was also examined. It is a scoping investigation that characterizes movement of agent simulants in several common construction materials and develops a sampling and analytical protocol that should be confirmed with experiments employing 'live' agents. Due to the high mammalian toxicity of warfare

Table 1
Simulants used in challenge tests

Simulant acronym	Chemical name	Chemical formula	CAS no.
DMMP[a]	Dimethyl methylphosphonate	$C_3H_9PO_3$	756-79-6
DIMP[b]	Diisopropyl methylphosphonate	$C_7H_{17}PO_3$	1445-75-6
CEES[c]	2-Chloroethylethyl sulfide	C_4H_9ClS	693-07-2

[a] Simulant for anticholinesterase agent VX; O-ethyl-S-2(diisopropylaminoethyl) methylphosphonothiolate, $C_{11}H_{26}NO_2PS$, CAS no. 50782-69-9.

[b] Simulant for anticholinesterase agent GB; O-isopropyl methylphosphonofluoridate, $C_4H_{10}FO_2P$, CAS no. 107-44-8.

[c] Simulant for the various formulations of vesicant sulfur mustard agents, H, HT, and HD; bis(2-chloroethyl)sulfide, $C_4H_8Cl_2S$, CAS no. 505-60-2.

agent compounds and the extraordinary precautions that must be followed during their experimental use, all tests reported here were conducted with chemical or physical analogues ('simulants') of each unitary agent: dimethylmethyl phosphonate ($C_3H_9PO_3$) or DMMP for agent VX, diisopropylmethyl phosphonate ($C_7H_{17}PO_3$) or DIMP for agent GB, and 2-chloroethylethyl sulfide (C_4H_9ClS) or CEES for the sulfur mustard formulations (see Table 1 for agent and simulant data). Note that while the chemical structures of VX and DMMP are dissimilar, DMMP is frequently used as a simulant for VX because both species are phosphonates, and have similar volatilities.

2. Materials and methods

A basic experimental design was followed, with a few alterations for temperature management, in all challenge tests. That is, a known concentration of agent simulant

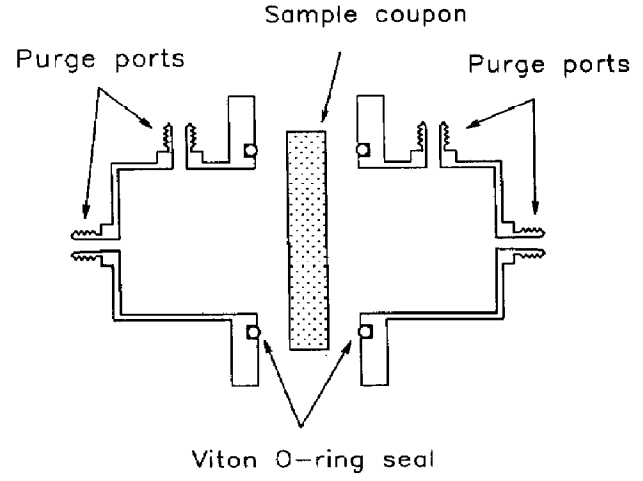

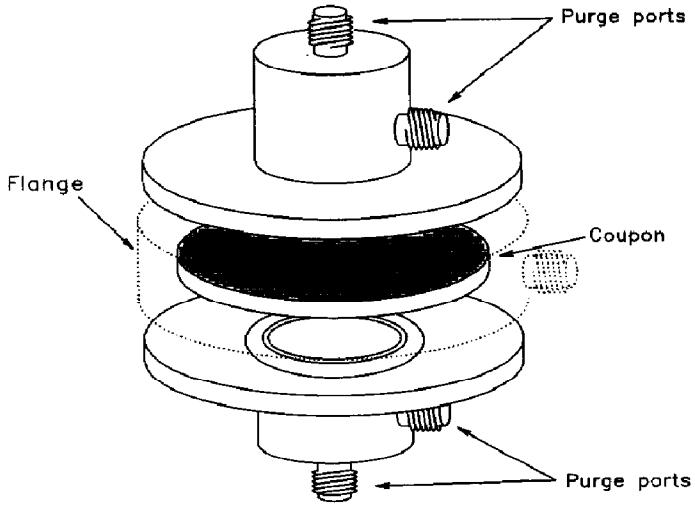

Fig. 1. Schematic diagram of test cell.

was applied to the surface (the 'spiked' face) of a sample coupon, after it had been mounted in a test cell with purge ports to the spiked space, breakthrough space and lateral space (see Fig. 1 for exploded schematic of test cell). Unpressurized air drawn through each of the three sample spaces 'swept' any simulant through the purge ports and into sorbent traps that were periodically removed, replaced, and analyzed for presence of simulant. The concentration of simulant used for each spike was derived from data documenting the maximum amount of undiluted nerve agent that elicited no toxic response in human subject tests ($\leqslant 6$ mg) [9,10].

The chemical agent simulants diisopropylmethyl phosphonate (DIMP) and dimethylmethyl phosphonate (DMMP), were obtained from Alpha Products (Ward Hill, MA 01835). Choroethylethyl sulfide (CEES) was obtained from Aldrich (Milwaukee, WI 53233). Test materials (the 'porous media' examined) were representative of local construction materials and included unpainted fir planks, gypsum wall board, unfaced brick, and concrete block. All were obtained from local construction supply vendors. Window glass was used as a non-porous reference material. Dimensions of sample wafers or 'coupons' are presented in Table 2.

2.1. Test cell

The test cell employed in this study is schematically illustrated in Fig. 1. Disassembled and assembled cell configurations are presented in Figs. 2 and 3. Each sample coupon of wood, wallboard, etc., was sandwiched between the two stainless steel plates of the test cell, and the test regions sealed with Viton® O-rings. The two steel plates were secured with C-clamps, and an outer flange enclosing the lateral space was clamped into place with an adjusting bolt (Fig. 3). This outer flange was sealed with a Teflon® gasket. There are two Swagelok® fittings for each sample region (spike, breakthrough, and lateral space). One was used as a fitting for the sorbent traps, and the other for an air inlet or outlet.

Changing the traps was relatively straightforward. The tubing connecting the trap to the flow system was removed, and the fitting holding the trap was loosened. The trap was removed, a fresh trap inserted, the fitting tightened, and the tubing reconnected. The entire process required approximately 45 s. A short time is essential for this operation to keep simulant loss from the airspace at a minimum. The amount of

Table 2
Dimensions of sample coupons used in challenge testing with warfare agent simulants

Material	Thickness (mm)	Diameter (mm)
Wood (unpainted fir)	20	65
Brick	19	55
Gypsum wall board[a]	13	65
Concrete block	25	55
Window glass	19	5153

[a] Includes paper coating on exterior and interior faces.

simulant collected in sorbent traps during challenge tests with glass was minimal in the breakthrough and lateral directions, indicating that the test cell was being assembled properly and that there was no significant simulant loss generated by the test cell design or manipulation.

Following each challenge test, the cell was disassembled and cleaned by sonicating in soapy water, rinsed, and cleaned with methanol. The cell was then heated at 100 °C for ca. 2 h before re-use.

The investigators considered 90 °F (32.2 °C) to be representative of local, elevated temperature conditions. The cell was thus maintained at a temperature that would keep air at the surface of the sample face at a constant 90 °F (32.2 °C). This was accomplished by wrapping the cell with electrical resistance heating tape wired to a variable voltage power supply. A thermocouple run through the air inlet to each sample space was positioned such that temperature measurements could be made in air immediately adjacent to the coupon surface. Room temperature (ca. 23 °C) experiments required no special temperature-maintenance procedures.

Undiluted simulants were spiked directly on the coupon face after each coupon was enclosed in its test cell. In some cases, experiments were performed by spiking a coupon with one simulant. For the more variable media (brick and concrete), DIMP and DMMP were simultaneously spiked, sampled, and analyzed for the same coupon.

Fig. 2. Disassembled test cell with Viton O-rings and purge ports installed.

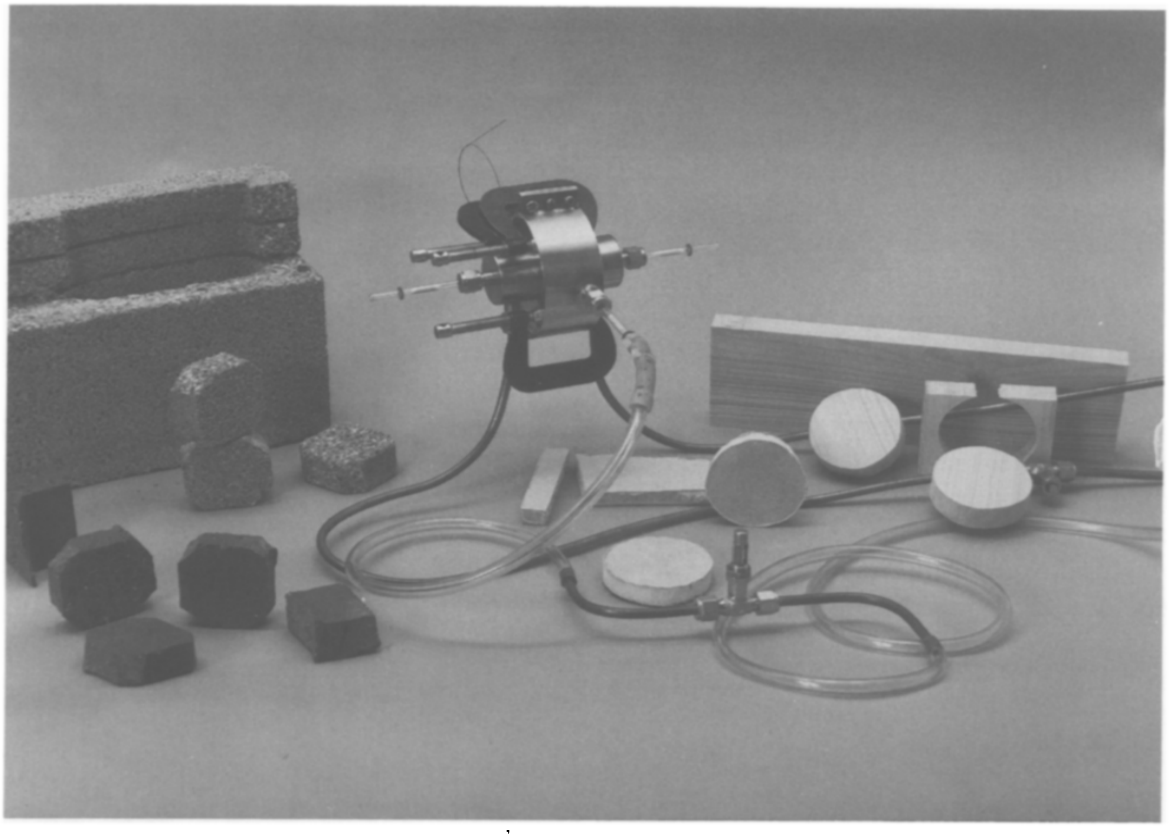

Fig. 3. Assembled test cell, with attached sorbent traps and sample lines. Porous media and test coupons of brick, concrete block, unpainted fir wood and gypsum wall board.

This 'double-spike' technique controlled for the irregular distribution of pores and channels among individual coupons of brick and concrete. Generally, one or two experiments were conducted for each temperature–simulant–matrix combination.

2.2. *Air sampling and flow determination*

Two different traps were used for the simulant experiments. For DIMP and DMMP, the depot area air monitoring system (DAAMS) tubes were employed. These are 6 mm o.d.75 mm long glass tubes filled with the sorbent Chromosorb 106. These were purchased from CMS Research Corp. (Birmingham, AL). For the experiments with CEES, tubes of the same size were packed with Tenax, a poly(*p*-2,6-diphenyl)-phenylene oxide (available from SKC South, Appomattox, VA).

Original consideration was given to using flows through the cell spaces equivalent to a linear velocity of 1 m/s. This is a velocity often used to characterize stable atmospheres when near-maximum inhalation doses are estimated from atmospheric model analysis [11]. However, the speed of 1 m/s would have resulted in a flow rate across the sample and breakthrough spaces of 68 l/min. There were several problems with this approach. Given the relatively small volume of the cell cavities, this would

have resulted in more than 10 air changes per second. At this rate, it was likely that the undiluted agent simulant would evaporate from the surface prior to any penetration of the porous media. Also, at such a flow rate, there was likely to be significant pressure drop across the sampling tube. The resulting pressurization of the cell may have led to unrepresentative movement of the simulant through the coupon. In addition, breakthrough of the simulants trapped on the DAAMS or Tenax tubes would be likely, especially at long sampling times. For these reasons, it was decided to use the lowest practical air flows through the sample cell (1–5 ml/min). At this low flow rate, evaporation of the simulant at the point of the spike would be minimized. In addition, low sampling flow rates would permit much longer sampling times without exceeding the capacity of the sorbent traps.

In some of the earlier experiments, air flow through the spiked and breakthrough spaces (and through the sorbent traps) was created using a pressurized cylinder of breathing air at a nominal rate of 2.5 ml/min. Air was pulled through the lateral space onto the traps using 'house' vacuum, at a rate of ca. 5 ml/min. Flow rate was determined at the beginning and end of each sampling period using a small bubble meter. Some variation in the flow rates over time were noted. This caused some concern, since even a modest change in the absolute flow rate at such low flows can result in a substantial relative change. Precise air flow measurements, together with accurate total flow volumes, are obviously vital to the realistic determination of simulant transport values. The very small air flow rates involved (2–6 ml/mm) in the spike, breakthrough, and lateral spaces of the test cell made accurate flow measurement by conventional manual techniques difficult and inaccurate. Later use of commercially available mass flow meters interfaced to ORNL-developed digital electronic integrators similar to those reported in Jenkins and Gayle [12] proved to be a superior method. Use of these integrators provided accumulated volumetric values accurate to better than $\pm 1.0\%$ in all cases.

The flow control and measurement arrangement ultimately employed for the experiments operated from a stabilized vacuum source, with three similar flow circuits for the three cell chambers. Each circuit pulled an air sample through the chamber sampling tube, into the mass flow meter, through a precision metering valve and on to the stabilized vacuum source. The three mass flow meters were Sierra model 821-2-10CC units (Sierra Instruments, Inc., Monterey, CA 93940). Stated accuracy of these units was $\pm 2\%$. However, they were calibrated to better than $\pm 0.25\%$ accuracy using a Buck model M-5 volumetric calibrator (A.P. Buck, Inc., Orlando, FL 32006). The vacuum source used in all tests was laboratory 'house vacuum' which normally varies from 508 to 711 Torr. Vacuum was stabilized at 381 Torr to provide a constant source for consistent manual flow rate control. To stabilize the vacuum for all three circuits, a single Conoflow model H-20VT-15 vacuum regulator (ITT/Conoflow Corp., St. George, SC 29477) was employed. Setting the desired flow rate was accomplished using a Nupro model B-SS4-VH precision metering valve (Nupro Division, the Swagelok Companies, Willoughby, OH 44049) in each circuit between the mass flow meter and the stabilized vacuum source.

The Sierra mass flow meters provide a local digital readout of flow rate, as well as a linear voltage output directly proportional to flow rate. Each of these three voltage

signals was channeled to the electronic integrator system referenced above. These units accept a voltage input and use a precision voltage-to-frequency circuit to drive a high-speed seven-digit electronic counter. The voltage signals were scaled so as to make the counter digits read directly in milliliters, the least digit being 0.01 ml. The overall combined accuracy of the components involved in the system provided a totalized (volume) accuracy of better than ± 1%. Periodic (every 21 days) recalibration was performed to verify this accuracy.

2.3. Analytical procedures

The GB and VX simulants (DIMP and DMMP, respectively) were simultaneously analyzed using on-column thermal desorption gas chromatography with phosphorus-specific flame photometric detection. The DAAMS tube was placed in a cold thermal desorber unit, and heated rapidly for 10 s to 220 °C. Helium carrier gas flowing at 28 ml/min swept the trap effluent onto the analytical column, which is a 30 m long0.53 mm i.d. DB-210 bonded phase fused silica capillary column. The flame photometric detector (FPD) was set in the phosphorus-specific mode at 525 nm. Hydrogen and air flow rates were 120 ml/min and 175 ml/min, respectively. The temperature program was an initial hold at 70 °C for 30 s, followed by an increase to 150 °C at the rate of 20 °C per minute. The final temperature was held for 5.0 min. Detector temperature was 200 °C. Elution time for the DMMP was 1.7 min, for the DIMP 1.24 min. Detection limits for DIMP and DMMP in this mode were ca. 0.2–0.3 ng on a Tracor model 540 chromatograph.

For CEES, the Tenax trap was placed in a cold thermal desorber unit, and heated rapidly for 15 s to 250 °C. Helium carrier gas flowing at 7 ml/min swept the trap effluent onto the analytical column, which is a 30 m long0.53 mm i.d., 1.0 μm film thickness DB-5 bonded phase fused silica capillary column. The flame photometric detector was set in the sulfur-specific mode at 393 nm. The hydrogen and air flow rates were 100 ml/min and 150 ml/min. The temperature program was an initial hold at 70 °C for 4 min, followed by an increase to 150 °C at the rate of 8 °C per minute. The final temperature was held for 2.0 min. Detector temperature was 200 °C. Elution time for the CEES was 7.9 min. The detection limit for CEES in this mode was ca. 1 ng with a Tracor model 540 chromatograph.

The DIMP extracts from concrete were analyzed using a gas chromatograph with phosphorus-specific thermionic detection. A 2 μl aliquot of extract was injected into the GC, with the injector held at 200 °C. Helium carrier gas flow was 3.3 ml/min through the analytical column, which is a 30 m long0.53 mm i.d. DB-23 bonded phase fused silica capillary column, with a 0.5 μm film thickness. Make-up gas flow was 30 ml/min. The thermionic detector was set in the phosphorus-specific mode. Hydrogen and air flow rates were 5.6 and 100 ml/min, respectively. The temperature program was an initial hold at 120 °C for 120 s, followed by an increase to 200 °C at the rate of 10 °C per minute. Detector temperature was 250 °C. The chromatograph used was a Varian model 3700. Elution time for the DIMP was 1.56 min.

2.4. Simulating decontamination

The effectiveness of decontamination was studied for glass as the reference material, and wood as the test medium. Technical Escort Operations of the US Department of the Army are governed by detailed guidance for the decontamination of materials [13]. These include both the exact composition of the decontamination mixture, the amount applied per unit area, and the procedure to be used. The Army specifies decontamination of glass with soapy water (at an unspecified concentration), and of wood with a slurry of high test hypochlorite (HTH). High test hypochlorite is commonly used as a chlorine source in swimming pools. Procedures specified in the Army guidance were scaled down, and applied to the test and reference materials.

Both the wood and glass coupons were spiked with 6 mg each of DIMP and DMMP outside the test cell. The spiked coupons were allowed to stand in a fume hood for 4 h, to approximate an estimated time for a decontamination unit to respond in an area outside the installation boundary. The glass surface was then flushed with ca. 30 ml of hot soapy water (prepared by dissolving 5 ml of Micro® soap in 100 ml water) and dried with a paper towel. The wood surface was decontaminated by application of 1.5 g of an HTH slurry (ca. 100 g of high test hypochlorite and 100 ml of water) to the 32.2 cm^2 surface with a plastic spoon. After allowing the slurry to stand on the spiked wood for 12–24 h (per Army protocol), the slurry was flushed away with ca. 100 ml of water. This process was repeated a total of three times. The coupons were then installed in individual test cells, and air samples taken over the course of a few days.

3. Results and discussion

3.1. Test cell

The cell depicted in Fig. 1 is the result of an optimization process based on several criteria. Principal criteria for cell design included: (1) The need to effectively seal three regions of the test coupon. These were the volumes adjacent to the spiked face of the coupon (sample space), the breakthrough space, and the volume adjacent to the 'raw' coupon edge (the lateral space). (2) The ability to change sorbent tubes rapidly and easily, yet minimizing cell complexity. (3) Ease of disassembly, decontamination, and cleaning of the cell. (4) Capacity for commonly available fittings and sealing materials.

Even so, isolation of specific regions of the test coupons was inexact; portions of the coupon surfaces which might otherwise be considered spike or breakthrough faces were actually isolated in the lateral space by the O-ring seal (see Fig. 1). Some confounding in data interpretation may have resulted. The investigators also realize that the porosity of tested materials did not permit perfect isolation of the various regions of the coupon by means of the flexible O-ring.

3.2. Analysis of DIMP and DMMP

Determination of airborne chemical agents and agent simulants through the use of the DAAMS tubes is a commonly accepted practice [14]. However, the methodology, while standard, was not particularly reproducible in our laboratory. Subsequent experiments indicated substantial variation in spike recoveries (ca. $\pm$ 50%) among individual DAAMS tubes. The spiking procedure itself was prone to variable performance. For example, protocols call for spiking methanolic solutions of the standards (DIMP and DMMP) on the interior wall of the glass tubing containing the Chromosorb 106, and drawing air through the tube to evaporate the solvent and draw the standard on to the sorbent. In such cases, recoveries of the spikes are $\geqslant$ 50%, but variable. However, if the sorbent bed itself is spiked, recoveries drop to ca. 5–10%. This erratic behavior of the sorbent collection devices may contribute to some of the apparent variability in the reported results.

3.3. Permeation

When breakthrough time is the parameter of comparison, it is clear that there is considerable variation in simulant behavior from coupon to coupon for the same medium (Tables 3–5). Given the range of observed concentrations (three to five orders of magnitude), the use of a specific absolute concentration level in the sample airspace to determine breakthrough time seemed inappropriate. In a few cases, it was apparent that more than one permeation mechanism was operative. For example, in one experiment with brick (Table 5), air concentrations of DIMP were greater than a factor of 10 or 100 above the detection limit in the lateral space immediately following the spike, diminished to near zero within 4 h, and then increased to more than a factor of 10^3 above the FPD detection limit of ca. 0.2–0.3 ng after a day or two. Use of a minimum detectible amount of simulant on the traps as indicating breakthrough would have been useful in some, but not all cases. For these latter situations, small concentrations (a few ng per trap) of simulants were found in immediately collected samples. At some later time, there was a pronounced increase in the airspace concentration of simulant. For the purpose of this study, the criterion for permeation was defined as a substantial change (usually a factor of four or greater) in the air concentration of the simulant, compared to the initial air concentrations. An additional criterion was that the substantial change in air concentrations had to be maintained for more than several hundred minutes. In some cases, permeation occurred so rapidly that the first air sample collected contained large amounts (hundreds of ng) of simulant. In practice, while the assignment of a breakthrough time was somewhat subjective, it was generally not difficult to discern when permeation had occurred.

Quantification of some high-concentration samples in individual sorbent traps was problematic. Collection of simulants on sorbent media, followed by thermal desorption gas chromatographic (GC) analysis, meant that the entire sample from an individual trap was introduced into the GC system at one time. Some traps contained as much as 100000 ng of simulant, which easily overloaded the flame photometric

Table 3
Simulant permeation through gypsum wall board

Simulant	Temperature (°F)	Breakthrough space			Lateral space		
		Permeation time (min)	Airspace concentration (μg/m³)		Permeation time (min)	Airspace concentration (μg/m³)	
			Initial	Maximum observed		Initial	Maximum observed
DIMP	72	270	62	2200	>11385	NA[a]	NA
DIMP	90	120	2200	81000	740	0.7	30
DIMP	90	120	210	126000	<60	383000	383000
DMMP	72	540	4	150	>8640	NA	NA
DIMP	90	120	2500	51000	300	0.7	1314
DIMP	90	120	260000	260000	<60	98000	98000
CEES	72	<40	299000	299000	<40	85500	120000
CEES	72	<30	104000	104000	30–60	27000	53000

[a]NA = not applicable.

Table 4
Simulant permeation through unpainted fir wood

Simulant	Temperature (°F)	Breakthrough space			Lateral space		
		Permeation time (min)	Airspace concentration (μg/m³)		Permeation time (min)	Airspace concentration (μg/m³)	
			Initial	Maximum observed		Initial	Maximum observed
DIMP	72	1560	0.4	0.5	1380	2.5	115
DIMP	90	>7250	NA[a]	NA	800	2500	2800
DIMP	90	>7200	NA	NA	410	20	340
DMMP	90	>7250	NA	NA	1820	146	5259
DMMP	90	>7200	NA	NA	>7200	27[b]	27[b]
CEES	72	>8612	NA	NA	<45	30000	30000
CEES	72	>6162	NA	NA	<15	20000	44000

[a] NA = not applicable.
[b] Peak concentrations were not achieved. Level decreased after initial high concentration.

Table 5
Simulant permeation through brick

Simulant	Temperature (°F)	Breakthrough space			Lateral space		
		Permeation time (min)	Airspace concentration (μg/m³)		Permeation time (min)	Airspace concentration (μg/m³)	
			Initial	Maximum observed		Initial	Maximum observed
DIMP	72	> 5485	NA[a]	NA	< 20	19	19
DIMP	72	> 10407	NA	NA	< 60	11300	95500
DIMP	72	> 17155	NA	NA	< 22	17400	17400
DMMP	72	> 4230	NA	NA	< 30	7	450
DMMP	72	> 17155	NA	NA	< 22	15710	15710

[a] NA = not applicable.

detector employed. This was particularly the case for simulant samples collected from the spiked space. In such cases, concentration estimates were made by performing a single point 'calibration'.

An approach to addressing this problem for future studies may be splitting the sample prior to collection or reducing the size of the spike. However, the presence of 'active sites' within the porous medium (see below) may mandate the use of a spike quantity which is sufficiently large so as to react with the active sites, with an excess remaining to migrate through the medium. Shortening the sampling period, so as to reduce the quantity of simulant collected on any one trap, would necessitate the collection of many more traps (factor of 10 to 100 more). Analysis of such a large number of traps may prove prohibitively expensive. An alternative to such an approach may be periodic sampling. For example, collection of a sample for 1 min out of every 10 min might be performed. However, if rapid changes in the air concentration of the simulants occur, such changes may be missed if periodic sampling is employed.

The most consistent breakthrough behavior was achieved with gypsum wall board. Permeation times for DIMP and DMMP into the breakthrough space of the wall board coupon were generally a factor of two to four less at 90 °F (32.2 °C) when compared to the times obtained at room temperature (ca. 23 °C). The range of observed maximum concentrations for DMMP varied over three orders of magnitude, from 150 (at 23 °C) to 260 000 $\mu g/m^3$ (at 32.2 °C). Permeation of the nerve agent simulants into the lateral space of the gypsum wall board was much less consistent. For individual experiments with DIMP and DMMP at 32.2 °C and all experiments with CEES, lateral permeation required less than 1 h. In some room-temperature experiments with DIMP or DMMP, no discernable lateral permeation occurred within one week. While it is tempting to attribute such breakthrough time differences to alterations in temperature, the authors believe that the small size of the existing data set precludes making a definitive conclusion. A concentration–time profile of DIMP migrating into the breakthrough space of gypsum wall board is presented in Fig. 4. The profile is typical of many of those for DIMP and DMMP in gypsum board. That is, initial permeation occurs within 2 h, followed by a concentration maximum within 10–20 h, rapid decline (in this case, to ca. 10 000 $\mu g/m^3$), and little further variation until termination of the experiment.

The summed total quantity of DIMP collected from both the lateral and breakthrough spaces of wallboard could account for only a fraction (10–30%) of the total mass (6 mg) of simulant originally spiked. Because the amount of simulant initially evaporating from the spiked face was so large, quantification was not practical with the measurement techniques employed. Thus, whether the mechanism for the rise and subsequent fall of the simulant concentrations in either the breakthrough or lateral space results from depletion of the available simulant reservoir due to evaporation from the spiked face, or retention of the remainder of the simulant by active sites within the coupon matrix can only be speculated at this time.

Permeation times were much less for CEES on gypsum wall board when compared to the data for DIMP and DMMP (Table 3). Penetration time into both lateral and breakthrough spaces was always less than 1 h. In addition, chromatographic analysis

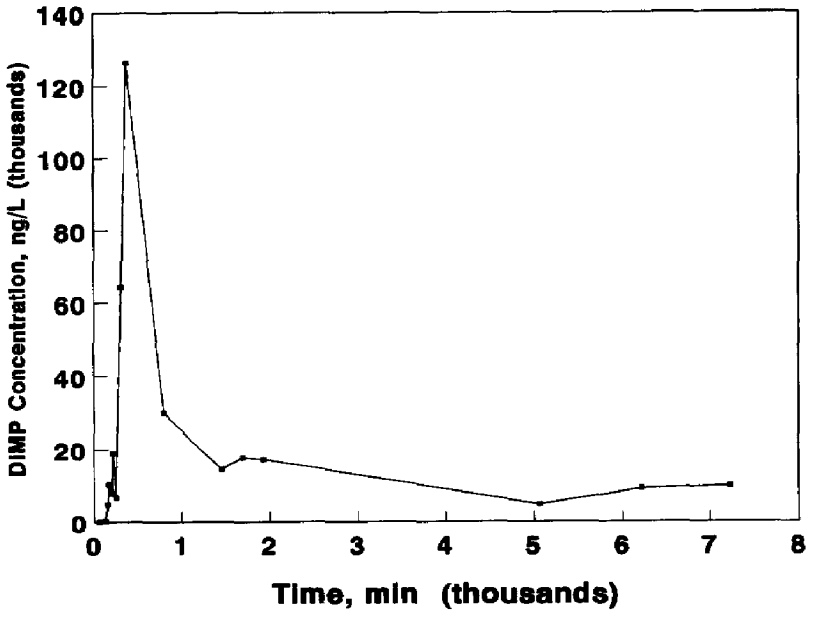

Fig. 4. Concentration–time profile of DIMP in breakthrough space of gypsum wall board following 6 mg spike. Breakthrough at 120 min; temperature, 90 °F.

of the airspace samples revealed a second constituent which eluted immediately prior to the CEES. This is suspected to be the CEES hydrolysis product 2-hydroxylethyl sulfide, which has been reported by other investigators [15]. However, no definitive analysis of this constituent was performed during the current study. The migration behavior of the suspected hydrolysis product tracked that of CEES. However, the concentration of the unknown constituent (assuming a similar response factor to that of CEES) in both lateral and breakthrough airspaces varied considerably. In one experiment, maximum airspace concentrations were comparable (50–100%) to those of CEES. In another, they were much less (2–10% of those of CEES). The CEES simulant seems to penetrate more rapidly (large variability, but maximum observed difference was over 200 times more rapidly; see Table 3) than DIMP or DMMP, perhaps due to its less polar nature.

The results for simulant spikes in unpainted fir wood coupons are reported in Table 4. In contrast to the gypsum wall board, simulant permeation to the breakthrough face of wood was not an important mechanism. Principally, simulants followed the wood grain and permeated into the lateral space. Permeation times in the lateral direction for DIMP varied from ca. 400 to 1400 min. Times were shorter at the elevated temperatures. Despite its chemical similarity to DIMP, the DMMP behaved differently and exhibited considerably longer permeation times. In one instance, significant lateral permeation of the DMMP did not occur within 120 h, at which time the experiment was terminated. For the DIMP and DMMP, maximum airspace levels in wood were lower by at least two orders of magnitude than the maximum levels achieved with gypsum wall board (see Table 3). As with the gypsum board, the CEES rapidly broke through (< 60 min) to the lateral space. No measurable level of CEES

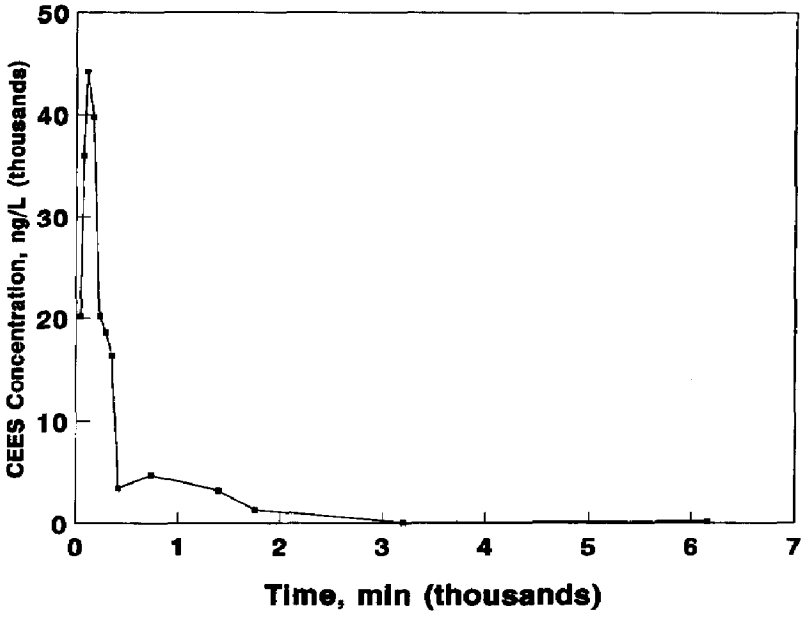

Fig. 5. Concentration–time profile of CEES in lateral space of wood, following 6 mg spike. Breakthrough at < 15 min; temperature, 72 °F.

was observed in the breakthrough space. The profile of CEES permeation into the lateral space of a wood coupon is presented in Fig. 5. As with the data presented for DIMP in the breakthrough space of gypsum board (Fig. 4), there was a rapid increase in the lateral space concentration of CEES, followed by a rapid decrease (usually in less than 15 h) and a relatively lower steady state concentration for days. The behavior of the suspected CEES hydrolysis product was somewhat different in wood (see Fig. 6). In one experiment (Expt. no. 16 in Fig. 6), it was similar to that of the CEES, both in quantity and profile. In a second experiment (Expt. no. 17), the constituent permeated at a lower, but much more constant rate.

Simulant movement through brick was determined only for DIMP and DMMP (Table 5). No simulant permeation to the breakthrough space was observed, even after nearly 12 days, while permeation into the lateral space usually occurred in less than 30 min. The data presented in Fig. 7 are typical, with the maximum lateral airspace concentration (ca. 16000 $\mu g/m^3$) achieved by the time of the first sampling, and a rapid decrease to a low, relatively steady state concentration (>1000 $\mu g/m^3$). This rapid lateral movement may be due to the high porosity of the medium.

Data characterizing DIMP and DMMP movement through concrete are portrayed graphically in Fig. 8. These simulants behaved quite differently. Whereas DIMP permeated into the lateral space at a relatively steady rate, DMMP achieved a maximum concentration (ca. 30 $\mu g/m^3$) very rapidly (within 4 h), followed by a rapid decrease in concentration to an approximate steady state level (at 22 h). In contrast to the brick, gypsum board, and wood, absolute lateral space concentrations of DIMP and DMMP in concrete were lower by as much as a factor of 1000 (i.e., 30 $\mu g/m^3$). In another experiment, spiking one-tenth the usual amount of DIMP on the surface of

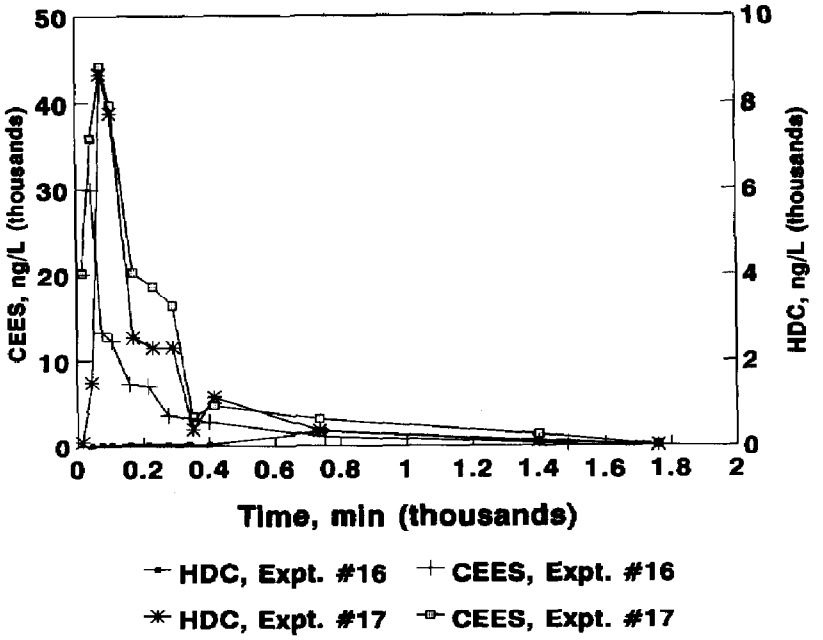

Fig. 6. Concentration–time profile of CEES and suspected CEES hydrolysis product in lateral airspace of wood. Temperature, 72 °F. (Data truncated at 2000 min to facilitate display. Note dual concentration scale.)

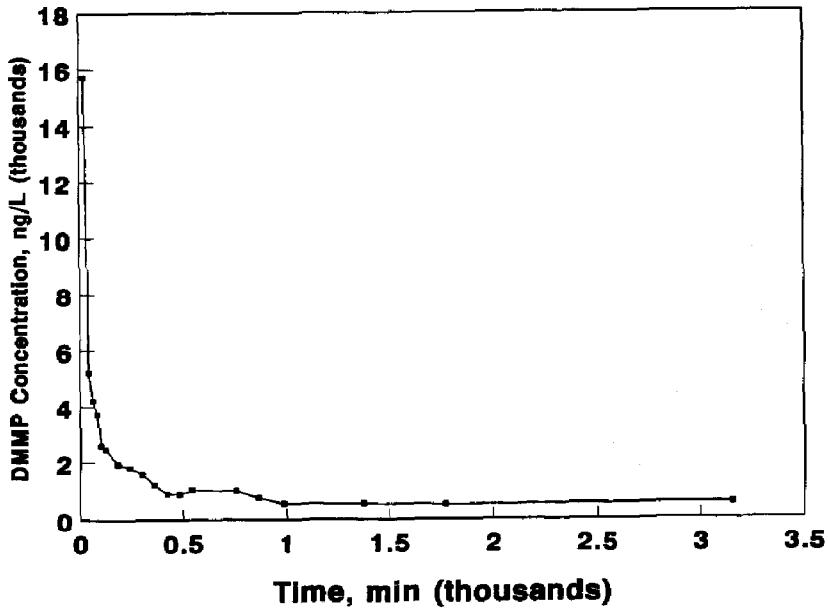

Fig. 7. Concentration–time profile of DMMP in lateral space of brick, following 6 mg spike. Breakthrough at < 22 min.

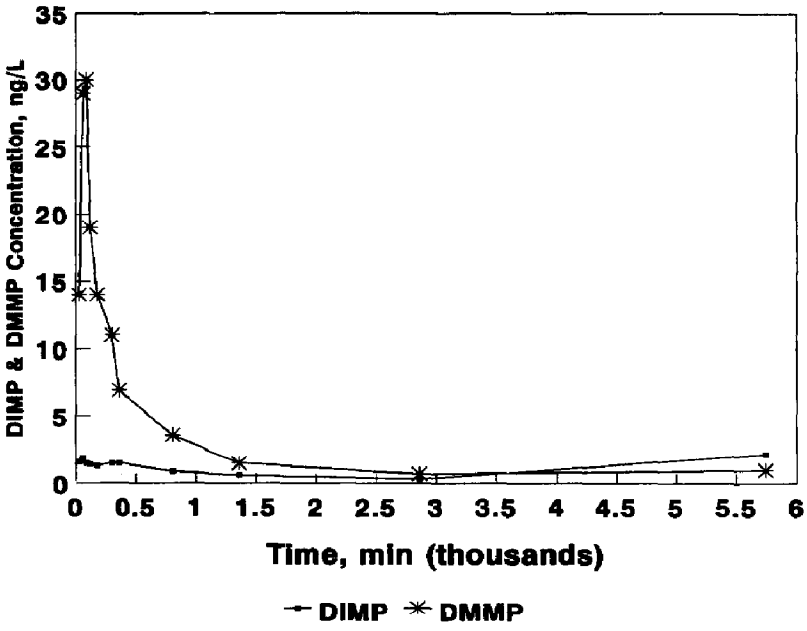

Fig. 8. Concentration–time profile of DIMP and DMMP in lateral space of concrete block, following 6 mg spike. Breakthrough at < 30 min.

the concrete resulted in no observable amount of simulant permeating to the lateral space in 96 h. Data from the low-spike experiment, coupled with the relatively small lateral space concentrations presented in Fig. 8, suggest that active sites that retain or react with DIMP and/or DMMP may exist within the concrete. Work performed at other laboratories suggests that chemical agents may be decomposed in concrete [16].

3.4. HTH decontamination

Decontamination experiments were limited to DIMP and DMMP on wood and glass because of the difficulty of generating reproducible results with concrete or brick coupons, the potential hydrolysis of the CEES, and the destruction of the paper coating that would occur during decontamination of gypsum board. Not surprisingly, decontamination of the glass was very effective. There was no simulant permeation into the lateral or breakthrough spaces, and only trace amounts of simulants (sub-nanogram quantities) in the spiked space. There were no detectable levels of DIMP/DMMP in the lateral or breakthrough spaces of wood following the decontamination procedures described above. The results of one decontamination experiment are presented in Fig. 9. Results for DIMP differ considerably from those of DMMP. While both simulants apparently de-gas from wood following decontamination (indicating the HTH decontamination procedure is not 100% effective on unpainted fir wood), DIMP attained a maximum spiked airspace concentration more slowly (see Fig. 9) and at a much lower level (30 vs. 800 $\mu g/m^3$). In contrast, the DMMP reaches its maximum concentration more rapidly, and at a much higher level (by a factor of 40), perhaps due to its greater volatility. These data suggest that the

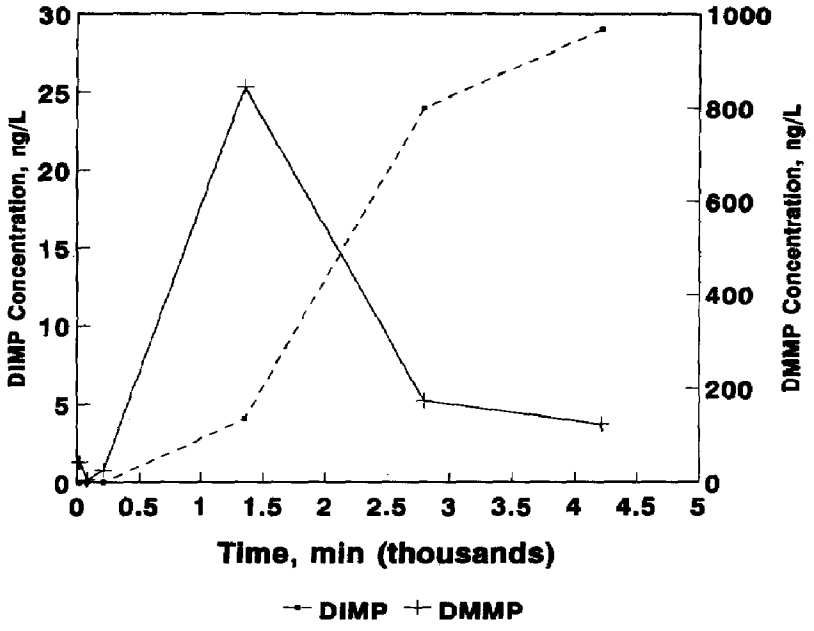

Fig. 9. Permeation to spiked space of DIMP and DMMP in wood after decontamination with HTH. Time 0 is 16–18 h after initial spike of 6 mg simulant.

HTH decontamination procedure may be more effective at removing DIMP, than DMMP, from wood.

During the HTH decontamination of wood experiment, the HTH slurry was allowed to continuously remain on the wood surface. No air monitoring of the sample space was performed during this period, so there are no data for use in determining if surface recontamination by agent simulants occurred during that time. The first air sample was collected within 20 min following the final decontamination rinse, and contained 44 $\mu g/m^3$ DMMP in the sample space. For the period of observation, sample space levels of DMMP attained a maximum of ca. 800 $\mu g/m^3$ at ca. 23.3 h. This value is ca. 15% of the maximum lateral space concentration attained during one breakthrough experiment of DMMP on wood.

The data for DIMP suggest that measurable recontamination of the wood surface began approximately 16 h following the final decontamination rinse. For the period of observation, sample space air concentrations of DIMP attained a maximum of 29 $\mu g/m^3$ at ca. 70 h, or ca. 25% of the maximum lateral space concentration attained during breakthrough experiments of DIMP on wood (at 72 °F).

3.5. Agent simulant recovery from test coupons

A number of approaches were examined for the recovery of simulants spiked onto test materials. Test protocols were evaluated for DIMP spiked on concrete as a worst case. Previous testing in our laboratory had suggested that DIMP would be absorbed

into the concrete matrix and little would migrate through the coupon. It was unknown, but suspected, that the DIMP was undergoing chemical reaction with constituents of the concrete and producing a non-permeating species. This phenomenon has been reported for VX and GB by others [16].

Initial tests with ground, spiked concrete in air met with limited success. Concrete was broken into several small pieces, and individual pieces placed in glass vials. Exactly 6 mg of DIMP in methanol solution (0.9 mg/ml) was spiked directly onto the face of a concrete chip. The vial was sealed for 2 h to permit penetration of the spike into the concrete.

Initial grinding tests were performed under water. To accomplish this, the spiked chip was further broken with a pointed chisel and hammer. All pieces were then placed in a mortar, covered with distilled water, and ground to a fine powder with a pestle. The water and ground concrete were extracted with 250 ml of methyl tertiary butyl ether (MTBE). The MTBE was separated from the aqueous phase using a separatory funnel. The aqueous phase was washed with excess MTBE in two 50 ml portions; the washes were added to the first 250 ml of MTBE extract. The volume of the resulting 350 ml solution was reduced to 10 ml under dry nitrogen. Results of this experiment are provided in Table 6.

To determine if losses of DIMP were occurring due to evaporation during processing, or reaction with the concrete, a series of experiments were performed in which some delay occurred following the sample spike, prior to addition of MTBE extractant. Following the addition of MTBE, the samples were allowed to stand overnight.

Table 6
Recoveries of DIMP following aqueous grinding and extraction with MTBE

Experiment no.	DIMP recovery (%)
1	Sample lost
2	75
3	53

Table 7
Recoveries of DIMP following delays in MTBE extraction

Sample no.	Time delay following extraction (h)	DIMP recovery (%)
1A	17	48
1B	17	51
2A	0.5	70
2B	0.5	67
3A	0	53
3B	0	51

To avoid artifactual evaporation, no volume reduction was performed and the extract was analyzed by GC as described below. Results of these experiments are reported in Table 7. The results of these two experiments suggested that extraction using MTBE in this manner could probably consistently achieve no greater than 50% recovery. As a result of the poor recoveries obtained, we developed a novel method employing Soxhlet extraction with an organic solvent.

The entire DIMP-spiked coupon of concrete was placed in the extraction thimble of a Soxhlet extraction system. Methyl *t*-butyl ether (MTBE) was the extraction solvent. The unit was heated and the extraction conducted for approximately 4 h. The extract was concentrated under dry nitrogen, and an aliquot analyzed using the method described below. Recovery of DIMP by this procedure was 94%. Time and resource limitations precluded further testing.

Note that the analytical procedure employed for the extract is quite different from the procedure previously described for analyses of DAAMS tubes. However, we consider that the DAAMS tube procedure could also be used by spiking an aliquot of the MTBE extract on a DAAMS tube, blowing off the solvent with dry helium, and analyzing the tube appropriately.

An accurate determination of the material balance with the described protocol would be difficult. A number of technical hurdles must first be addressed. Ideally, to determine the material balance, one should merely add the amount of simulant collected on all of the DAAMS tubes from all of the air spaces (sample, breakthrough, and lateral) over the course of the experiment, and then perform an extraction of the 'used' coupon. However, as was noted above, the quantities evaporating from the spiked face of the coupon are so large as to be beyond the quantifiable range of the analytical method. And, despite the apparent high concentrations of simulants present in the lateral or breakthrough spaces observed (as much as several hundred thousand $\mu g/m^3$), the absolute quantities of simulants collected represent a very small fraction of the total amount of material spiked. For example, total quantities of simulants collected typically ranged from 1–500 μg, which represents 0.02–8% of the total spike. And while Soxhlet extraction of the coupons would appear to be capable of removing most (95% of DIMP observed) of the remaining simulant in the coupon, this approach has only been tested once, and at a relatively short elapsed time between spiking and extraction. It is unknown whether this approach would be as effective at one week past the spike time.

The stability of the simulant, or lack thereof, may also confound determination of an accurate material balance. There is very clear evidence that the CEES decomposes significantly during the experiment, because the decomposition product is chromatographable under the conditions of the analysis. In the case of CEES, it would seem relatively straightforward to identify the decomposition product and quantify it. However, there may be other simulant decomposition products which are not easily chromatographed. An accurate determination of material balance would require a more extensive analysis of the coupons to confirm, identify, or refute, the presence of simulant decomposition products. However, even optimistic assessments suggest that more extensive appraisal will be capable of accounting for no more than 85–90% of the total spike mass.

4. Conclusions

Procedures and experimental apparatus for determining permeation rates of three chemical warfare agent simulants through wood, gypsum wall board, brick, and concrete have been developed. Data indicate that simulant permeation through wood is nearly always in the lateral direction and follows the wood grain. The simulant CEES penetrates wood more rapidly (<1 h) than DIMP (7–20 h) or DMMP (30–120 h). Despite application of a constant simulant spike, there was much variability in maximum lateral space concentrations. Wood lateral space concentrations of DMMP ranged from 27 to 5300 $\mu g/m^3$, from 115 to 2800 $\mu g/m^3$ for DIMP, and from 30 000 to 44 000 $\mu g/m^3$ for CEES. Decontamination of DIMP and DMMP from the wood surfaces with large amounts of HTH slurry was not completely effective under the experimental protocol evaluated.

All simulants permeated to the breakthrough space of gypsum wall board in a matter of a few hours. The simulant CEES permeated more rapidly (< 1 h) than the other simulants. Maximum breakthrough space concentrations ranged from a low of 150 $\mu g/m^3$ (DMMP at $\approx$ 23 °C), to a high of nearly 300 000 $\mu g/m^3$ (CEES at $\approx$ 23 °C). Permeation into the lateral space was also substantial, but the time required for lateral permeation and maximum sample space concentrations to develop were highly variable, even for a single simulant.

The simulants DIMP and DMMP permeated the lateral space of brick within 1 h. No breakthrough space concentrations were detected for the > 91 h period of observation.

In the single experiment of cinder block challenged with DIMP and DMMP, both penetrated into the lateral space within 4 h. Breakthrough airspace levels of DMMP and DIMP were much lower than those found in the lateral space. Additional replicates of this experiment are needed.

Data indicate that there is substantial sample-to-sample variation in individual coupons of porous media, particularly brick and concrete, which have been tested. For definitive results with a particular medium, large numbers of individual coupons may need to be challenged. Overall, if the agents behave comparably to that of the simulants tested, the data suggest that permeation into porous building materials is relatively rapid (within hours). Decontamination of wood with HTH slurries does not appear to be entirely effective. The difficulty of mass balance determination prevented accurate estimation of decontamination effectiveness. Findings suggest that more effective decontamination in porous media could be attained if decontamination mixtures were formulated to penetrate porous media as effectively as the agents themselves.

5. Acknowledgements

This research was performed for the US Department of the Army, Office of the Assistant Secretary of the Army (Installations, Logistics and Environment) under Interagency Agreement DOE No. 1769-1354-A1 by the Oak Ridge National

Laboratory, Oak Ridge, TN 37831, managed by Martin Marietta Energy Systems, Inc., for the US Department of Energy under contract No. DE-AC05-84OR21400.

The authors wish to thank Dr. J. Richard Ward, Acting Director, Research and Technology Directorate, US Army Edgewood Research and Development Engineering Center at Aberdeen Proving Ground, MD, for critical advice and insight.

6. References

[1] S.A. Carnes and A.P. Watson, Disposing of the US chemical weapons stockpile: An approaching reality, JAMA, 262 (1989) 653–659.

[2] S.A. Carnes, Disposing of chemical weapons: a desired end in search of an acceptable means, Environ. Prof., 11 (1989) 279–290.

[3] S.A. Carnes, NEPA compliance for the Chemical Stockpile Disposal Program, Environ. Prof., 11 (1989) 434–446.

[4] A.P. Watson, K.R. Ambrose, G.D. Griffin, S.S. Leffingwell, N.B. Munro and L.R. Waters, Health effects of warfare agent exposure: implications for stockpile disposal, Environ. Prof., 11 (1989) 335–353.

[5] A.P. Watson and N.B. Munro, Reentry planning: The technical basis for offsite recovery following warfare agent contamination, ORNL-6628, Oak Ridge National Laboratory, Oak Ridge, TN, 1990.

[6] M. Buchanan, R. Hettich, L. Waters, J. Caton, J.X. Xu and A. Watson, Rapid method for low-level detection of chemical warfare agent simulants in agricultural media (in ORNL review).

[7] US Department of the Army, Safety regulations for chemical agents H, HD, HT, GB, and VX, AMC-R 385-131, Headquarters, US Army Material Command, Washington, DC, 1987.

[8] E.M. Speirs, NATO's preparations for chemical warfare, in: E.M. Speirs (Ed.), Chemical Warfare, University of Illinois Press, Urbana, IL, 1986, pp. 142–174.

[9] D. Grob, B. Zeigler, G. Saltzer and G.I. Johnston, Further observation on the effects in man of methyl isopropyl fluorophosphonite (GB): Effects of percutaneous absorption through intact and abraded skin, MLCR 14, DA-18-108-CML-3014, Johns Hopkins University and Hospital, Baltimore, MD, 1953.

[10] R.A. Jenkins, M.V. Buchanan, R. Merriwether, R.H. Ilgner, T.M. Gayle, J.H. Moneyhun and A.P. Watson, Protocol for determination of chemical warfare agent simulant movement through porous media, ORNL/TM-12002, Oak Ridge National Laboratory, Oak Ridge, TN, 1992.

[11] R.L. Miller and F.C. Kornegay, Downwind doses from potential releases associated with the chemical stockpile disposal program, Environ. Prof., 11 (1989) 315–323.

[12] R.A. Jenkins and T.M. Gayle, An instrumental inhaled smoke dosimeter for the quantitative characterization of aerosol exposures, in: C.L. Sanders, F.T. Cross, G.E. Dagle and J.A. Mahaffey (Eds.), Pulmonary Toxicology of Respirable Particles, Proc. 19th Ann. Hanford Life Sciences Symp., Richland, WA, CONF-791002, DOE Technical Information Center, Springfield, VA, 1980, pp. 68–86.

[13] Department of the Army, Technical Escort Operations, Report FM 3-20, Headquarters, US Department of the Army, Washington, DC, 1981.

[14] W. Fowler, Research Staff, Southern Research Institute, Birmingham, AL, transcribed telephone conversation with R.A. Jenkins, 18 August 1992.

[15] Y.C. Yang, J.R. Wood and T. Luteran, Hydrolysis of mustard derivatives in aqueous acetone–water and ethanol–water mixtures, J. Org. Chem., 51 (1986) 2756–2759.

[16] E.R. Zamejc, E.J. Mezey, T.L. Hayes, D.K. Wetzel and B.C. Garrett, Development of novel decontamination techniques for chemical agents (GB, VX, HD) contaminated facilities, Report AMXTH-TE-TR-85012, US Army Toxic and Hazardous Materials Agency, Aberdeen Proving Ground, MD, 1985.